An Adaptive Three-Phase UPS Inverter Controller

L.G. Barnes III and R. Krishnan
Motion Controls System Research Group
The Bradley Department of Electrical Engineering
Virginia Polytechnic Institute and State University
Blacksburg, Virginia 24061
Phone: 703-231-4311 Fax: 703-231-3362
e-mail: kramu@vtvm1.ccvt.edu

Abstract - Linear and nonlinear adaptive control strategies for a three-phase uninterruptible power supply (UPS) inverters are described. Without a priori knowledge of the UPS system parameters, the adaptive controller synthesizes an internal input/output digital controller mapping which minimizes the instantaneous load voltage waveform errors relative to the sinusoidal load voltage command. An on-line adaptive learning algorithm is described which promotes steady-state controller stability. Results of computer simulations and experiments using this adaptive control technique are presented.

I. INTRODUCTION

Sinusoidal voltage uninterruptible power supplies (UPS) are designed to supply low-distortion, regulated sinusoidal voltages to critical loads such as data-processing, communication, and medical electronics systems. A typical solid-state UPS system is depicted in Fig. 1. Pulse Width Modulation (PWM) techniques are typically utilized to control the inverter switching pattern where the inverter output voltage fundamental and harmonic components are controlled through the output voltage waveform switching angles [1][2]. The output filter circuit is designed to suppress unwanted inverter output voltage harmonic components. The UPS inverter switching pattern is controlled in a closed-loop system with the objectives of compensating for battery bank DC voltage variations and output filter series inductance voltage drops and phase-shifts created by the load currents. Inverter control techniques described in [3] through [7] have been devised to achieve a fast-response to sudden load current changes and harmonic currents generated by nonlinear loads.

A time-optimal switching strategy described in [3] utilizes nonlinear feedback and inverter switching frequencies in the 10 to 100 KHz range. The use of nonlinear feedback makes the control system robust and less sensitive to load disturbances and output filter circuit parameter variations. Switching delays and losses limit the use of this control technique to low-power, single-phase UPS systems.

A single-phase UPS dead-beat control technique described in [4] utilizes a digital controller algorithm based on the output filter circuit discrete-time state transition equations.

Improvements in the dead-beat control technique are described in [5] through [7]. In order to eliminate steady-state load voltage errors created by mechanisms such as controller processing and inverter switching delays, output filter circuit parameter variations, inverter switching distortion effects described in [8][9], fixed-point controller operations, and DC voltage variations, the dead-beat controller is augmented with closed-loop load voltage error compensation in the form of either a proportional-integral (PI) controller or a repetitive controller described in [5]. In [6] and [7], a dead-beat controller for a three-phase inverter utilizing an inner inverter output current dead-beat control loop is described. In order to generate the inverter output current command each controller sampling period, prediction of the load current at the end of the sampling period is necessary. The performance of this dead-beat control technique depends largely on the quality of the inner current loop and the load current prediction method.

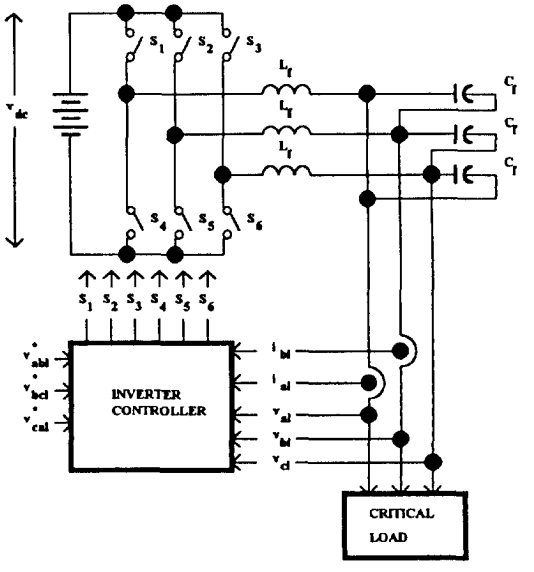

Fig. 1. Three-Phase UPS System

0-7803-2730-6/95 $4.00 © 1995 IEEE

In contrast to time-optimal switching strategy, dead-beat control techniques utilize constant and lower inverter switching frequencies making the application of these control techniques feasible in medium- and high-power UPS systems. On the other hand, the dependence of a dead-beat control technique on a priori knowledge of the output filter circuit response characteristics makes the performance of this technique sensitive to output filter circuit parameter variations.

In this paper, alternative UPS inverter control strategies in the form of linear and nonlinear adaptive controllers are described. As in the case of the time-optimal switching strategy, adaptive UPS inverter controllers display robust performance in a time-variant environment with uncertain characteristics. Without using closed-loop load voltage error compensation in the form of either a PI or a repetitive controller, or load current prediction as described in [6] and [7], the adaptive controller synthesizes a controller forward transfer function which minimizes the instantaneous load voltage waveform error relative to the load voltage command. In steady-state, the controller forward transfer function approximates the inverse transfer characteristics of the inverter/output filter system.

The nonlinear adaptive controller utilizes a multi-layer neural network or a neural network with one or more internal layers. The linear adaptive controller utilizes a neural network without internal layers. The adaptive controllers described in this paper are also referred to as neurocontrollers.

Adaptive control algorithms are described in Section II of this paper. Section III describes results of experiments run using the adaptive controller. Conclusions are given in Section IV.

II. Adaptive Control Of Ups

A. Adaptive Control Concept

The adaptive UPS controller is a digital feed forward controller containing gain coefficients that are updated by a learning process designed to optimize the controller's response to a desired performance criterion. The adaptive controller consists of two distinct parts: a feed forward control function which inputs load currents and voltages, and processes this information to produce the inverter output voltage commands $\{v^*_{di}(k),v^*_{qi}(k)\}$ expressed in the stationary d-q frame; and an on-line controller learning process which adjusts the feed forward controller gain coefficients with the objective of improving the controller's performance. k denotes the discrete-time index. The controller inputs are defined as follows:

$$x_1(k) = v^*_{dl}(k) \tag{1}$$

$$x_2(k) = v^*_{ql}(k) \tag{2}$$

$$x_3(k) = i_{dl}(k) - i_{dl}(k-1) \tag{3}$$

$$x_4(k) = i_{ql}(k) - i_{ql}(k-1) \tag{4}$$

where $\{v^*_{dl}(k),v^*_{ql}(k)\}$ are the load voltage commands expressed in the stationary d-q frame, and $\{i_{dl}(k),i_{ql}(k)\}$ are the sampled d-q frame load currents. A diagram of this adaptive controller is depicted in Fig. 2.

B. Controller Algorithms

The inverter output voltage commands are generated from controller inputs using one of two feed forward controller structures. One feed forward control structure utilizes a neural network with a single internal or hidden layer. The following equations describe the feed forward transfer characteristics of this control structure:

$$h_p(k) = \sum_{i=1}^{4} w^{(1)}_{pi}(k)\cdot x_i(k) \tag{5}$$

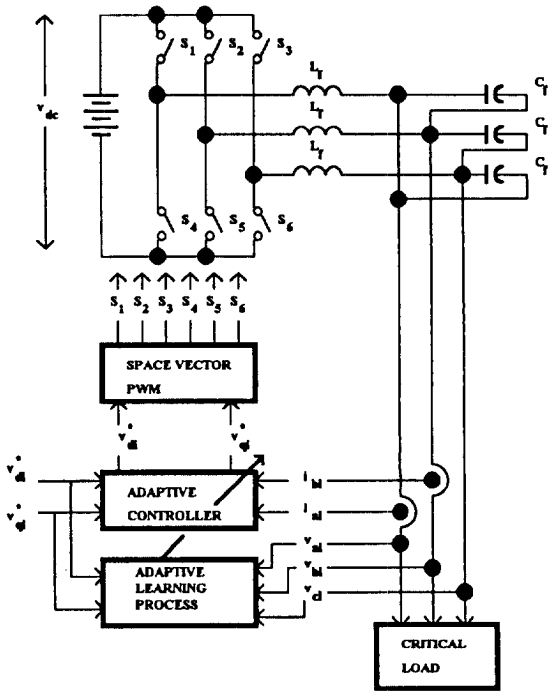

Fig. 2. Adaptive Control System

$$y_j(k) = \sum_{p=1}^{Q} w^{(2)}_{jp}(k) \cdot \tanh[h_p(k)] \quad (6)$$

$$v^*_{di}(k) = y_1(k) \quad (7)$$

$$v^*_{qi}(k) = y_2(k) \quad (8)$$

where $w^{(1)}_{pi}(k)$ and $w^{(2)}_{jp}(k)$ are the controller's gain coefficients or weights, and $h_p(k)$ is the p^{th} of Q hidden layer outputs. The other feed forward control structure utilizes a network without hidden layers. The following equation describes the feed forward transfer characteristics of this control structure:

$$y_j(k) = \sum_{i=1}^{4} w^{(3)}_{ji}(k) \cdot x_i(k) \quad (9)$$

where $w^{(3)}_{ji}(k)$ is a controller weight.

In order to eliminate the instantaneous load voltage errors

$$\varepsilon_{dv}(k) = v^*_{dl}(k) - v_{dl}(k) \quad (10)$$

$$\varepsilon_{qv}(k) = v^*_{ql}(k) - v_{ql}(k) \quad (11)$$

the controller's feed forward transfer characteristics approximate the inverse transfer function of the PWM inverter/output filter system. In addition to the linear output filter inverse transfer function on which conventional dead-beat controllers are based, the controller feed forward transfer characteristics include compensation for controller processing and inverter switching delays and other non-ideal system operating conditions such as inverter switching distortion effects and controller fixed-point operations. Using an adaptive feed forward control structure and a performance criterion defined by the sampled cost function

$$J(k) = \tfrac{1}{2} \cdot [\varepsilon^2_{dv}(k) + \varepsilon^2_{qv}(k)] \quad (12)$$

the feed forward transfer function is synthesized by an on-line learning process with the objective of minimizing the cost function defined in (12).

C. Operation of the Closed Loop System with the Proposed Controller

Controller sampling and program execution are synchronized to the PWM inverter switching pattern. The controller sampling rate is twice the inverter switching frequency. Inverter output voltage commands are converted to inverter switching commands using the space vector PWM process described in [10]. The operation of the closed-loop control system is outlined as follows:

i.) At the beginning of the sampling interval, $t = k \cdot T$, load voltage commands, currents, and voltages are sampled. T denotes the controller sampling period.

ii.) The instantaneous load voltage errors are computed and utilized in the controller learning process. Network weights are adjusted by the learning process. A limiter function is included in the learning process which prevents a weight fixed-point value overflow condition.

iii.) The inverter output voltage commands are generated using the controller inputs and the feed forward control function defined in either (5) and (6) or (9). Inverter switching commands are generated from the inverter output voltage commands using the space vector PWM process.

iv.) The switching commands are executed in the inverter during the following interval, $(k + 1) \cdot T \le t < (k + 2) \cdot T$. Load voltages sampled at $t = (k + 2) \cdot T$ result from the learning process and feed forward control function executed in the $k \cdot T \le t < (k + 1) \cdot T$ sampling interval.

Using a variation of the steepest descent method, network weights are modified by the learning process by step changes which are proportional to the cost function gradient $\delta J/\delta w$, where w denotes a network weight. This gradient is approximated in a fashion described by the equation

$$\delta J/\delta w = -c(k) \cdot [\varepsilon_{dv}(k) \cdot \delta v^*_{di}(k)/\delta w + \varepsilon_{qv}(k) \cdot \delta v^*_{qi}(k)/\delta w] \quad (13)$$

where c(k) is a small positive scalar known as the controller's learning-rate parameter. Two sets of network weights are utilized: one set utilized during even sampling intervals; and the other set utilized during odd sampling intervals. The gradients $\{\delta v^*_{di}/\delta w, \delta v^*_{qi}/\delta w\}$ are evaluated during the k^{th} controller sampling interval using the controller's network state in the $(k - 2)^{th}$ controller sampling interval.

The change in the network weights as a result of the controller's learning process is described by the equation

$$w(k) = w(k - 2) + \delta w(k) \quad (14)$$

where $\delta w(k)$ is the weight step change. Changes in the adaptive controller's output trajectory which result from the weight step changes are denoted as $\{\delta v^*_{di}(k), \delta v^*_{qi}(k)\}$. In order to avoid a cost function descent to a minimum defined by the conditions

$$\delta J(t)/\delta t = 0 \text{ and } J(t) > 0, \quad (15)$$

where t is the time variable, weight step changes are made in a fashion described by the equations

$$\text{sgn}[\delta v^*_{di}(k)] = \text{sgn}[\varepsilon_{dv}(k)] \quad (16)$$

$$\text{sgn}[\delta v^*_{qi}(k)] = \text{sgn}[\varepsilon_{qv}(k)] \quad (17)$$

$$\text{sgn}(a) = 1 \text{ for } a \geq 0 \quad (18)$$

$$\text{sgn}(a) = -1 \text{ for } a < 0. \quad (19)$$

In the learning process developed for the adaptive UPS controller, the polarity of a weight step change is determined logically from the polarity of the corresponding product term in the summations described in (5), (6), and (9) and the polarity of the network weight before modification. The magnitude of the weight step change is the absolute value of the gradient defined in (13). In the single-layer network learning process, the polarity of each product term change resulting from the weight step change is equivalent to the polarity of the corresponding d-q frame load voltage error. A similar technique is applied in the hidden-to-output layer weight modification routines for the neural network with a single hidden layer. In order to illustrate this method of weight modification, the following pseudo C programming language source code listing of the weight modification routine utilized in the network without a hidden layer is presented:

```
if(w(3)ji(k − 2)·xi(k − 2) ≥ 0.0)
{
  w(3)ji(k) = w(3)ji(k − 2) + c(k)·εj(k)·|xi(k − 2)|·
                sgn[w(3)ji(k − 2)];
}
else
{
  w(3)ji(k) = w(3)ji(k − 2) − c(k)·εj(k)·|xi(k − 2)|·
                sgn[w(3)ji(k − 2)];
}                                                    (20)
```

$$\varepsilon_1(k) = \varepsilon_{dv}(k) \quad (21)$$

$$\varepsilon_2(k) = \varepsilon_{qv}(k). \quad (22)$$

The input-to-hidden layer weight modification process in the neural network with a single hidden layer is performed using the conventional steepest descent algorithm. Weight step changes are computed in a fashion described by the equation

$$\delta w^{(1)}_{pi}(k) = \{\sum_{j=1}^{2} \varepsilon_j(k)\cdot w^{(2)}_{jp}(k-2)\}\cdot \text{sech}^2[h_p(k-2)]\cdot x_i(k-2). \quad (23)$$

Using this controller technique, the inverter output voltage command trajectory is modified each controller sampling interval in the direction indicated by the load voltage error vector $[\varepsilon_{dv}(k),\varepsilon_{qv}(k)]$. The load voltage trajectory reaches and converges to the desired trajectory described by the load voltage commands.

III. Experimental And Theoretical Results

A. Description of the UPS System Simulations and Experiments

The performances of the nonlinear and linear adaptive controllers were evaluated using computer simulations of a three-phase UPS system. The simulation parameters are given in the Appendix. Results obtained from UPS system experiments and simulations using balanced-passive, unbalanced-passive, and nonlinear three-phase loads are given in [11]. The results of UPS experiments and simulations with a nonlinear load are presented. The nonlinear load is an uncontrolled three-phase rectifier with a L-C output filter and resistive load.

The controller portion of the simulation utilized fixed-point math operations and an eight-bit analog-to-digital conversion process. The space vector PWM process was also performed using fixed-point math. The simulation was constructed with the objective of emulating the operation of the experimental controller utilized in the UPS system experiments. A 0.066 controller learning-rate parameter value was used in the simulations and in the later experiments.

The number of hidden layer outputs in the network utilized in the nonlinear controller was six. Ideally, increasing the number of hidden layers and hidden layer outputs improves the ability of a multi-layer neural network to synthesize nonlinear functional relationships. Given the limited precision of practical digital controllers, the improvement in neural network learning performance realized by increasing the network size is limited. In this neural network application, the selection of six hidden layer outputs corresponded to this practical limitation.

The initial network weights in the network without hidden layers were $w^{(3)}_{11}(0) = w^{(3)}_{22}(0) = 1.0$ with the remaining weights set to zero. The initial weights in the network with a

single hidden layer were randomly selected from a set of values in the range {−0.1,+0.1}. Additionally, inputs to this neural network were scaled down by a gain factor of 1/10. Network outputs were scaled up by a gain factor of 10.

B. Theoretical Results

Simulations were run with zero initial load currents and voltages. Steady-state simulation results were obtained after 30 inverter modulation frequency periods. Table 1 displays the load voltage spectral information results from the simulations using the nonlinear and linear adaptive controllers. Additionally, an open-loop simulation was run where the load voltage commands were directly utilized as the inverter output voltage commands. Table 1 results have been normalized with respect to the commanded load voltage magnitude.

Both controllers perform identically with regard to regulating the load voltage fundamental frequency component. The load voltage magnitude in steady-state is nearly equal to the commanded load voltage magnitude.

C. Experimental Results

In Fig. 3, the open- and closed-loop instantaneous load voltage errors measured in the nonlinear load experiments are depicted. As shown in Fig. 3, a significant reduction in the instantaneous load voltage errors is realized when the controller learning process is enabled. The on-line learning process does not create controller instability despite the use of load current feedback containing significant harmonic components and an output filter design with a pole located at a frequency which is lower than the load current harmonics.

Due to the similar performances of the nonlinear and linear adaptive controllers, further study of the adaptive control concept was made using the linear adaptive controller algorithms in an experimental three-phase UPS system. Data displayed in Fig. 3 was obtained from nonlinear load experiments using the linear adaptive control algorithm programmed in a microprocessor-based inverter controller.

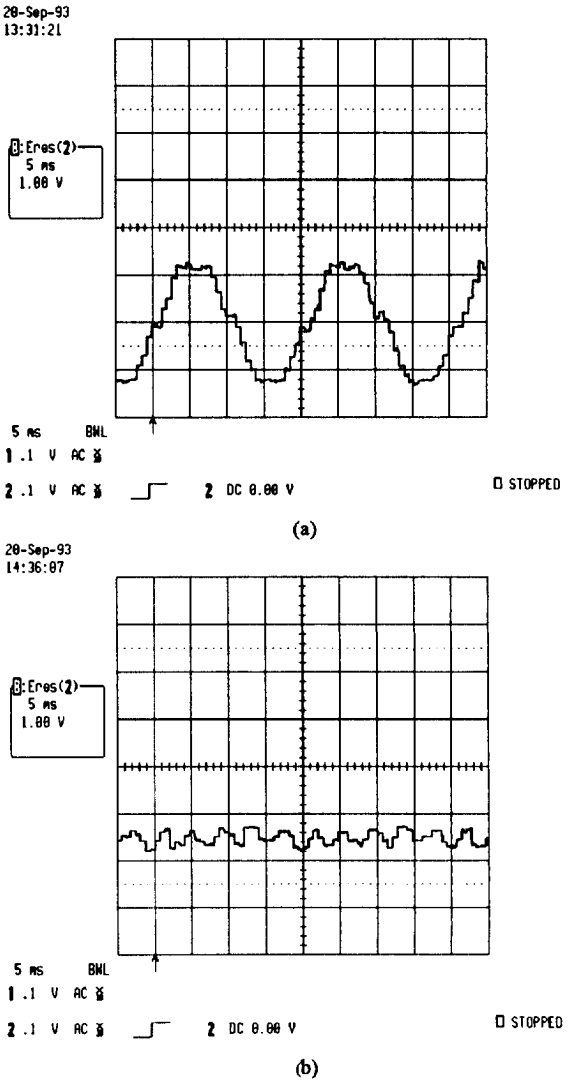

Fig. 3. Experimental measurements of load voltage errors in the (a) open-loop and (b) closed-loop control experiments; a nonlinear load was connected.

TABLE 1
Load Voltage Spectral Data From Nonlinear Load Simulations

Harmonic	Open-Loop P.U.	Linear Adaptive P.U.	Nonlinear Adaptive P.U.
1	1.107	0.997	0.997
5	0.047	0.043	0.049
7	0.017	0.013	0.021
11	0.023	0.024	0.031
13	0.012	0.001	0.015
17	0.011	0.005	0.013
19	0.003	0.003	0.001
23	0.001	0.001	0.003
25	0.003	0.001	0.004

Fig. 4 depicts experimental measurements of the instantaneous load voltage errors and the DC link voltage. The DC link voltage was varied from 200 to 150 volts with the controller learning process enabled. A balanced-passive three-phase load was connected.

Load voltage compensation is made through the controller's learning process. The peak load voltage error

with a 200 volt DC link was in the order of 0.03 p.u. where the commanded load voltage magnitude is the normalization constant. The load voltage error was reduced as the DC link voltage was reduced. This error reduction was due to the improved inverter output voltage spectral characteristics at higher inverter output voltage commands. This response continued until the link voltage is reduced to 165 volts. Below 165 volts, the load voltage errors increased. Due to the insertion of inverter switching dead time, load voltage compensation with the DC link voltage below 165 volts was not achieved.

Fig. 5 depicts experimental measurements of the instantaneous load voltage errors and the load current during a 100% step increase of three-phase load. The step increase of load current was created by connecting additional resistive load in the form of incandescent filament lamps. The cold filament resistance of the lamp load is somewhat lower than the hot filament resistance, and consequently, the initial step load application was greater than 100%. The controller learning process was enabled during this experiment.

The response to the additional resistive load began approximately one cycle prior to the rise of load current. The delay in the load current increase is created by the output filter's response to the step decrease in load impedance. Prior to the rise of load current, load voltage error compensation was performed by the modification of the network weight values during the controller learning process. After the rise of load current, additional error compensation was obtained from load current feedback fed forward in the single-layer network. Based on the measured load voltage errors, the controller response time after the rise of load current was approximately one and one-half cycles.

The results of experiments involving DC link voltage variation and step load application verify the ability of this adaptive control technique to minimize the instantaneous load voltage errors given dynamic UPS system conditions. Stable controller operation is achieved over the entire range of DC link voltage variation including the range below 165 volts where linear inverter output voltage control was not possible. A stable controller response was also achieved in the step load experiment despite the initial low resistance of the added load and subsequent nonlinear load resistance transition to the hot filament resistance.

IV. Conclusions

The following contributions to the author's belief are considered original:

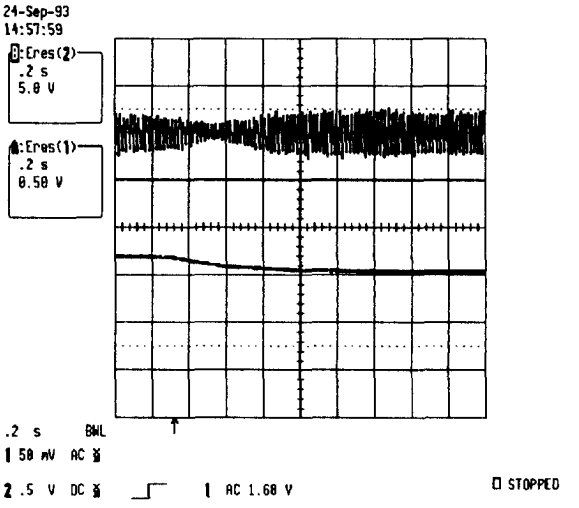

Fig. 4. Load voltage instantaneous errors (top trace) verses the DC Link voltage (bottom trace).

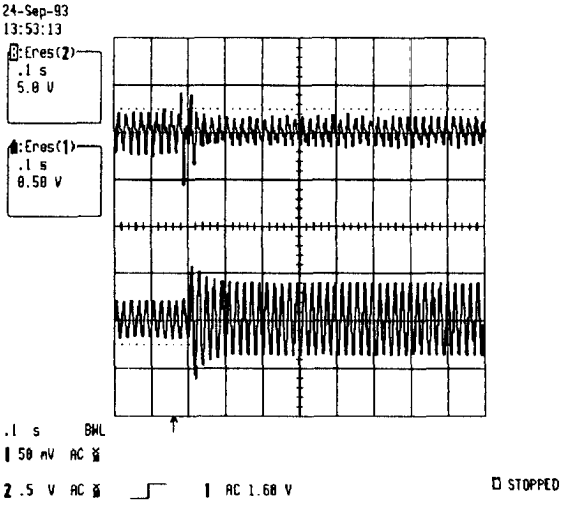

Fig. 5. Load voltage instantaneous error (top trace) verses load current (bottom trace): 100 % load increase with controller learning process enabled.

i.) An adaptive controller for UPS inverter control is proposed, simulated, and experimentally verified for the first time.

ii.) The core controller design is independent of UPS system parameters such as inverter modulation and switching frequencies, output filter design, and component values. Characteristic of nonlinear controllers, the adaptive controller is relatively insensitive to system parameter variations and modeling errors. Unlike conventional nonlinear controllers, the adaptive controller can operate effectively at relatively low sampling rates or inverter switching frequencies.

iii.) Load voltage waveform phase delays associated with controller computational delays and the load voltage synthesis process in the output filter circuit are inherently compensated. Though conventional linear controllers can be designed to compensate for such delays, the controller design is based on inverter/filter system parameters which are particular to the UPS application and subject to uncertainties such as output filter component tolerances or accurate prediction of load current feedback.

The performance of the controller utilizing a multi-layer neural network appeared to be no better than the performance of the controller utilizing a network without hidden layers. The capability of the multi-layer neural network to synthesize a fixed nonlinear input/output mapping is not utilized in this application.

V. Appendix

The three-phase UPS parameters utilized in the experiments and simulations are listed as follows:

Commanded Line-to-Line Load Voltage	= 106 volts @ 50 Hz.
Nominal DC Link Voltage	= 200 volts
Inverter Switching Frequency	= 750 Hz.
Inverter Switching Dead Time	= 60 μs.
Output Filter Series Inductance	= 10 mH.
Output Filter Line-to-Line Capacitance	= 45 μF

References

[1] Hasmukh S. Patel and Richard G. Hoft, "Generalized Techniques of Harmonic Elimination and Voltage Control in Thyristor Inverters: Part I-Harmonic Elimination", IEEE Trans. On Industry Applications, Vol. IA-9, No. 3, pp. 310-317, May/June 1973.

[2] Hasmukh S. Patel and Richard G. Hoft, "Generalized Techniques of Harmonic Elimination and Voltage Control in Thyristor Inverters: Part II-Voltage Control", IEEE Trans. On Industry Applications, Vol. IA-10, No. 5, pp. 666-673, September/October 1974.

[3] Atsuo Kawamura and Richard G. Hoft, "Instantaneous Feedback Controlled PWM Inverter with Adaptive Hysteresis", IEEE Trans. on Industry Applications, Vol. IA-20, No. 4, pp. 769-775, July/August 1984.

[4] Kalyan P. Gokhale, Atsuo Kawamura, and Richard G. Hoft, "Dead Beat Microprocessor Control of PWM Inverter for Sinusoidal Output Waveform Synthesis", IEEE Trans. on Industry Applications, Vol. IA-23, No. 5, pp. 901-910, September/October 1987.

[5] Toshimasa Haneyoshi, Atsuo Kawamura, and Richard G. Hoft, "Waveform Compensation of PWM Inverter with Cyclic Fluctuating Loads", IEEE Trans. on Industry Applications, Vol. 24, No. 4, pp. 582-589, July/August 1988.

[6] Takao Kawabata, Takeshi Miyashita, and Yushin Yamamoto, "Dead Beat Control of Three Phase PWM Inverter", IEEE Trans. on Power Electronics, Vol. 5, No. 1, pp.21-28, January 1990.

[7] Takao Kawabata, Takeshi Miyashita, and Yushin Yamamoto, "Digital Control of Three Phase PWM Inverter with LC Filter", IEEE Trans. on Power Electronics, Vol. 6, No.6, pp.62-72, January 1991.

[8] Ira J. Pitel, "Spectral Errors in the Application of Pulse Width Modulated Waveforms", IEEE Trans. on Industry Applications, Vol. IA-17, No. 3, pp. 289-295, May/June 1981

[9] P.D. Evans and P.R. Close, "Harmonic Distortion in PWM Inverter Output Waveforms", IEE Proceedings, Vol. 134, Pt. B, No. 4, pp. 224-232, July 1987.

[10] Heinz Willi Van Der Broeck, Hans-Christoph Skudelny, and Georg Viktor Stante, "Analysis and Realization of a Pulsewidth Modulator Based on Voltage Space Vectors", IEEE Trans. on Industry Applications, Vol. 24, No. 1, pp. 142-150, January/February 1988.

[11] L. G. Barnes III, "Voltage-Source Inverter Output Waveform Compensation Using Adaptive Intelligent Control", Ph.D. dissertation, Virginia Polytechnic Institute and State University, Blacksburg, Va., May 1994.